

Very High Kr^{7+} Rydberg States after Electron Capture from Laser-Excited $\text{Rb}^*(17p)$ Atoms into Kr^{8+}

A. Pesnelle,¹ R. Trainham,¹ J. Pascale,¹ E. Monnard,² and H. J. Andrä³

¹ *Service des Photons, Atomes et Molécules, CEA, Centre d'Etudes de Saclay, 91191 Gif-sur-Yvette-Cedex, France*

¹ *Laboratoire des Ions, Atomes et Agrégats, CEA, CEN Grenoble, 38054 Grenoble-Cedex 9, France*

¹ *Laboratoire de Spectrométrie Physique, CNRS, Université Grenoble I, 38402 St. Martin d'Hères-Cedex, France*
and *Institut für Kernphysik, Universität Münster, 48149 Münster, Germany*

(Received 18 January 1995)

State selective measurements of single electron capture in collisions at 40 and 18 keV of multicharged ions Kr^{8+} with laser-excited $\text{Rb}^*(17p)$ have been performed by use of a new field ionization detector. We have observed very highly excited states $\text{Kr}^{7+}(n)$, as a result of the high degree of excitation of the target and of the high charge of the projectile. Wide n distributions of the cross sections have been obtained experimentally, with n ranging from 67 to 110. By using the classical trajectory Monte Carlo method, we have calculated even wider n distributions, in contrast to the extended classical over-barrier model which yields much narrower n distributions.

PACS numbers: 34.50.Rk, 34.60.+z, 34.70.+e

Alkali-metal atoms, laser excited to high Rydberg levels, represent unique targets with a very weakly bound electron well differentiated from the rest of the core electrons and are especially suited for a pure process of single electron capture. Because of the major role played by the initial binding energy of the electron to be captured, and also by the high charge of the projectile [1], very high ionic n orbitals are populated. In this paper we report the first experimental observation of the final n dependence of cross sections for electron capture from laser-excited $\text{Rb}^*(17p)$ Rydberg atoms by highly charged Kr^{8+} ions. To date, n -state distributions after capture from laser-excited $\text{Na}^*(nl)$ Rydberg atoms have been observed via field ionization of neutrals in collisions with singly charged Ar^+ and Na^+ ions by MacAdam and co-workers [2]. In contrast to field ionization of Na^* or Ar^* atoms, field ionization of Kr^{7+} multiply charged ions is complicated by the sensitivity of the trajectories to any field, including the ionizing field itself; this is the fundamental experimental difference between the present experiment and that of MacAdam and co-workers. A previous experiment with O^{6+} used fluorescence photon detection from $\text{O}^{5+}(n = 10 \rightarrow n = 8)$ to observe alignment effects on the capture from $\text{Na}^*(3p)$ [3]. He^{2+} projectiles have also been employed for the same kind of alignment experiments on $\text{Na}^*(3p)$ by use of translational energy spectroscopy [4].

Capture from the $\text{Rb}^*(17p)$ Rydberg level, with an electron binding energy of ≈ 0.066 eV, yields wide n distributions in the final $\text{Kr}^{7+}(n)$ ion with most probable orbitals of $n \approx 75-80$, with mean radii ranging up to the nanometer scale, $\bar{r} \approx 60$ nm, and with lifetimes estimated at more than several microseconds. These states are semiclassical in nature so that the capture process, which takes place at distances as large as 130 nm and has total cross sections of the order of 10^{-10}

cm^2 , can well be described by the three-body classical trajectory Monte Carlo (CTMC) method [5]. In our CTMC calculations model potentials have been used to simulate the interaction between the active electron and the ionic Rb^+ and Kr^{8+} cores [6].

The experiment is carried out in an apparatus with three crossed beams, which will be described in detail in a forthcoming paper. In short, a high brilliance beam of charge and mass analyzed Kr^{8+} ions at $E_0 = 40$ or 18 keV is delivered by the Accelerator of Multicharged Ions (AIM) in Grenoble [7]. In the interaction zone, the ions perpendicularly intersect a beam of Rb atoms, laser excited to the $17p$ level by uv radiation at 301.6 nm. The uv beam, of about 10 mW, is generated by second harmonic generation in a cw ring dye laser operated with rhodamine-6G and an ammonium dihydrogen crystal [8] and is anticollinear with respect to the ion beam. The strongest hyperfine component of the ^{85}Rb line $5s^2S_{1/2}(F = 3) \rightarrow 17p^2P_{3/2}$ at $33\,158.54\text{ cm}^{-1}$ is used for excitation. The fluorescence from the cascades is monitored by a photomultiplier with a color filter and is used as a control during the Kr^{7+} ion detection.

After single electron capture, the Kr^{7+} ions leave the interaction region with an energy $E'_0 = E_0 - eV_i$, where V_i is the potential of the interaction region. They are then separated from the rest of the ion beam by a first electrostatic spectrometer and enter a cylindrically symmetric electrostatic field ionizing lens system of 11 electrodes. This ionizing lens, with an axial field collinear to the ion beam, has been designed to yield a constant transmission, especially when charge-changing ionization takes place. A simulation of the ion trajectories through the lens and the downstream diaphragms, including the field ionization process at different positions along the lens axis, yields a transmission of 80% with deviations less than 3%. The lens creates, on its axis, a symmetrically decreasing neg-

ative potential $U(z) = -cz^2$ towards its center. Consequently, the ions experience an electric field $F(z) = 2cz$, linearly increasing from 0 at the lens entrance to $F_m = 9.1$ or 5.2 kV/cm near the center where it is inverted, and linearly decreasing again to 0 at the lens exit.

When an ion in a Rydberg state n_i is field ionized at the critical field $F_i = 2cz_i$, with the corresponding potential $U_i = -cz_i^2$, the resulting Kr^{8+} loses kinetic energy of eU_i when leaving the ionizing lens. A kinetic energy shift results, therefore, from electron loss within the lens. The energy distribution of these Kr^{8+} ions is measured with a second electrostatic spectrometer by scanning its voltage. The abundance of Kr^{8+} ions at the energy $E'_0 - eU_i$ corresponds to that of Kr^{7+} ions with a Rydberg electron in level n_i .

An energy spectrum of the product Kr^{8+} ions for a collision energy of 40 keV is shown in Fig. 1, together with a simulation of the ion spectrum using our CTMC n distribution. Without laser excitation, the ion signal disappears completely to a nearly negligible constant background signal. All the data show the same overall behavior, but we do observe systematic shifts in our ion spectra depending upon the initial state of Rb ranging from $15p$ to $25p$. In the present Letter, we focus our interest upon the $17p$ and will present the other results in a forthcoming paper. Rydberg levels with high n in Kr^{7+} show up close to E'_0 , i.e., in the highest energy part of the ion spectrum, whereas those with lower n at lower energies. The narrow peak close to E'_0 stems from very high Rydberg levels which are ionized near a small diaphragm at the entrance of the ionizing lens. The diaphragm produces, over the first few millimeters of the lens, a sharp increase of the axial field before the

potential decreases significantly. All Rydberg levels with n above a certain value are field ionized in this region and show up within a very narrow band of energies. The peak contains levels $n \geq 110$ for $F_m = 5.2$ kV/cm, or $n \geq 94$ for $F_m = 9.1$ kV/cm, except those already ionized in the first electrostatic spectrometer located before the ionizing lens.

The experimental cross section is obtained using the critical field of the classical field ionization model $F_c(n) = q^3/16n^4$, the transformation from F_c to ion energy as outlined above, and taking into account the constant resolution $E/\delta E$ of the energy analyzer. The results of this procedure for four spectra at 40 keV at different experimental conditions are shown in Fig. 2. A coefficient of 9 instead of 16 in the classical field ionization formula, as a consequence of the shifts of the Stark states [9], would correspond to higher $F_c(n)$, and would shift and slightly broaden the distribution in Fig. 2 to higher n values, up to the $n = 77-124$ range.

Our CTMC n distributions are calculated with a sufficient number of trajectories to provide statistical uncertainties less than 5% near the maximum and less than 10% at the edges. The distribution at 40 keV, presented in Fig. 2, extends from $n \approx 40$ to 250, with a maximum at $n \approx 73$ corresponding to a cross section $\sigma_{\text{th}} \approx 6.7 \times 10^{-13}$ cm² (note that the total capture cross section is 6×10^{-11} cm²). In comparison, the experimental $\sigma_{\text{ex}}(n)$ exhibits its maximum at $n \approx 78-80$, falls off faster than $\sigma_{\text{th}}(n)$ for $n > 95$, and also decreases faster than $\sigma_{\text{th}}(n)$ for $n < 70$.

The experiment has been repeated with the same collision partners at a collision energy of 18 keV. The results are shown in Fig. 3 together with our CTMC

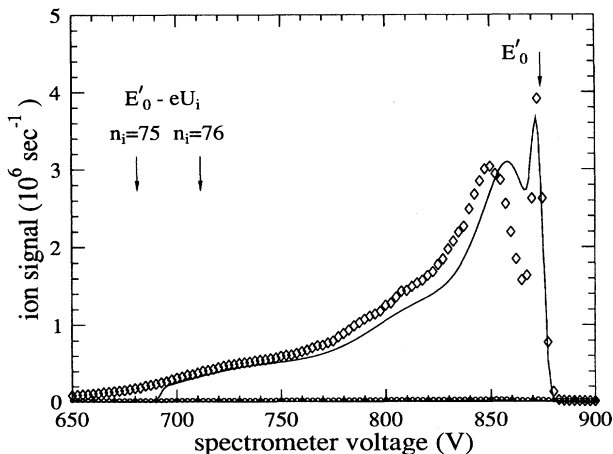


FIG. 1. Kr^{7+} ion spectra for capture from $\text{Rb}^*(17p)$ into Kr^{8+} at 40 keV, with $E_0 = 48$ keV, $V_i = +1$ kV, and $F_m = 5.2$ kV/cm; \diamond , laser on; \circ , laser off. Kr^{7+} ions are detected as Kr^{8+} ions after field ionization. The ion kinetic energy is related to the spectrometer voltage by $54 \times V + 8$ (eV). Continuous line: ion signal simulated by using the CTMC n distribution.

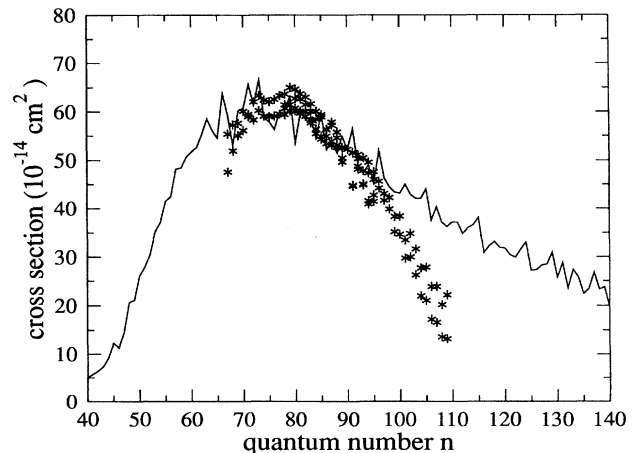


FIG. 2. Experimental cross section $\sigma_{\text{ex}}(n)$ for capture from $\text{Rb}^*(17p)$ into Kr^{8+} at 40 keV vs quantum number n defined within the classical field ionization model, *'s. The CTMC capture cross section $\sigma_{\text{th}}(n)$ calculated for each value of n is represented by a continuous line. The cross section σ_{ex} has been normalized to the CTMC calculations at $n = 90$.

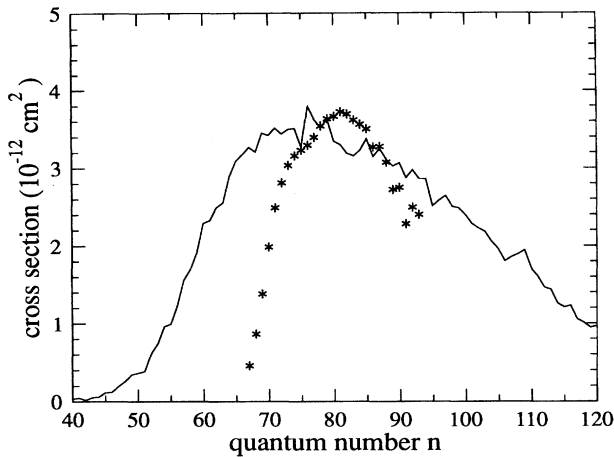


FIG. 3. Experimental cross section $\sigma_{\text{ex}}(n)$ for capture from $\text{Rb}^*(17p)$ into Kr^{8+} at 18 keV vs quantum number n defined within the classical field ionization model, *'s. The CTMC capture cross section $\sigma_{\text{th}}(n)$ calculated for each value of n is represented by a continuous line. The cross section σ_{ex} has been normalized to the CTMC calculations at $n = 75$.

calculations for this energy. The CTMC n distribution extends from $n \approx 44$ to 180, giving a total cross section of 10^{-10} cm^2 . We observe that $\sigma_{\text{ex}}(n)$ has its maximum at $n \approx 80-82$, while that of $\sigma_{\text{th}}(n)$ is at $n \approx 76$, and falls off faster than $\sigma_{\text{th}}(n)$ for higher and lower values of n . Our experimental data tend to indicate a decrease of the distribution width between 40 and 18 keV as shown by our CTMC calculations which yield a decrease of the width by a factor of ≈ 1.8 . However, $\sigma_{\text{ex}}(n)$ has a width smaller than $\sigma_{\text{th}}(n)$ for 18 keV (by a factor of ≈ 2), and to a lesser extent for 40 keV. For both collision energies 18 and 40 keV, $\tilde{v} = v_p/v_e$ is 1.33 and 1.99, where v_p is the projectile velocity and v_e the initial orbital velocity of the excited electron, and fulfills the condition $1 \leq \tilde{v} \leq 4$ for which the CTMC method is generally assumed to be valid [5]. In comparison, the extended classical over-barrier model (ECB) [10] yields positions of maxima close to our data ($n \approx 80$ for 18 and 40 keV), but n distributions much narrower than the experimental ones (by factors of ≈ 3 and 4, respectively), and all the more than the CTMC distributions. It is worth noting that the ECB model has never been used for such target atoms, excited in Rydberg levels, and its application here is just indicative.

The $\sigma_{\text{ex}}(n)$ distributions derived from our data rely on several approximations discussed in the next three paragraphs.

The classical field ionization model attributes an ionization probability of 1 as soon as the electric field exceeds the classical $F_c(n)$ and zero if it does not. This notion of a discontinuous threshold is useful [9], albeit not exact since it ignores tunneling ionization. Quantum mechanical calculations of the F -dependent ionization probability $\Gamma(F, n_+, n_-, m_l)$ for Rydberg states of hydrogen, with all l

values, actually show very strong variations with the field strength (e.g., for $n = 30$, Γ increases by 8 orders of magnitude for a field increase of 22%) [11]. For given experimental conditions of observation period and slew rate this appears as “pseudo” thresholds, generally at fields higher than that given by the classical formula $F_c(n) = q^3/16n^4$. This has been observed after laser excitation of specific high n , low l states [12]. If we extrapolated a similar behavior to the present case, it would result in a shift of our $\sigma_{\text{ex}}(n)$ distribution to higher n values with a slight broadening. One can therefore assume that the shape of the $\sigma_{\text{ex}}(n)$ distribution is not much affected by the choice of the function $F_c(n)$ but that its position is sensitive to it. An exact determination of the position would require the calculation of the ionization probability $\Gamma(F, n_+, n_-, m_l)$ of all Stark substates for the present n, l, m_l distributions. The l, m_l distributions are not accessible in our experiment, but our CTMC calculations yield these distributions for the total capture process. The m_l distributions for both energies are peaked at $m_l = 1$, but are quite broad; they decrease nearly exponentially to $1/e$ at $m_l \approx 18$, and extend up to $m_l \approx 47$. With such distributions, the determination of the exact Γ would be a huge task.

The Kr^{7+} ions are accelerated towards the center of the ionizing lens in order to ensure constant transmission, which would vary strongly for a decelerating system. Consequently, the lowest n , which is ionized deep inside the ionizing lens, experiences a slew rate of the electric field about twice as high as the one for the highest n at the entrance of the ionizing lens. Compared to the huge variations of Γ with F , this should not have a strong effect and should not reduce considerably the detection efficiency of the low n states.

At 40 keV, the transit time between the target region and the ionizing lens is $\approx 1.3 \mu\text{s}$, so one must consider the lifetimes of the $\text{Kr}^{7+}(n)$ ions. An n -scaling law ($\tau \propto n^{4.5}/q^4$, averaged over statistical populations of l sublevels), based on hydrogenic lifetimes [13], suggests that the signal of the lowest n levels could be underestimated due to their short lifetimes [$\tau(n = 67) \approx 2.5 \mu\text{s}$]. However, a nonstatistical population of l sublevels, such as the CTMC one, could modify these averaged lifetimes. The CTMC l distribution of the total capture cross section is compared in Fig. 4 with the l distribution calculated with a statistical population of l sublevels weighted by the present CTMC n distribution for both energies. Sublevels with $l \leq 15$ [$\tau(n = 67, l = 15) \approx 1.6 \mu\text{s}$] are nearly not populated, and for $l \leq 45$ at 18 keV and for $l \leq 52$ at 40 keV still remain underrepresented [$\tau(n = 67, l = 45) \approx 14 \mu\text{s}$ and $\tau(n = 67, l = 52) \approx 18 \mu\text{s}$]. Thus we can conclude that $\tau(n = 67, \text{averaged over all } l) \gg 14 \mu\text{s}$, in particular, when noting $\tau(n = 67, l = 60) \approx 24 \mu\text{s}$ at the maximum of the l distribution at 18 keV. These l -specific lifetimes of the shortest lived n state detected in the experiment, $n = 67$, are estimated from the hydrogenic specific- l lifetimes [14] and the n -scaling law

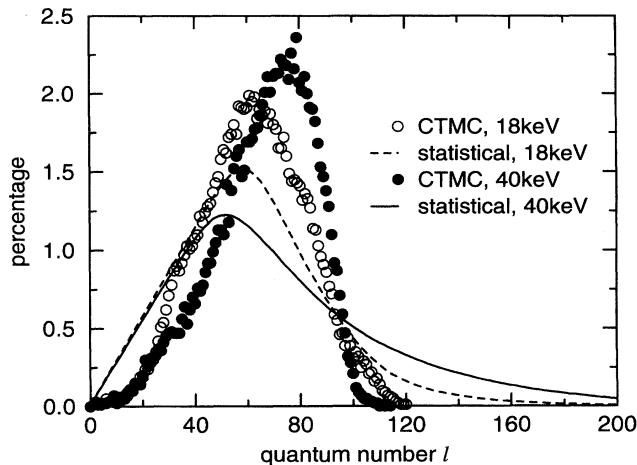


FIG. 4 Distributions of l sublevels for the total electron capture from $\text{Rb}^*(17p)$ into Kr^{3+} at 18 and 40 keV, calculated by the CTMC method, or determined from the CTMC calculated n distribution and assuming a statistical population of l sublevels.

$\tau \propto n^3/q^4$. Since all $\tau(n \geq 67, l \geq 60)$ are still longer, we neglect the effect of the transit time from the target to the ionizing lens.

In conclusion, we have observed very high Rydberg levels, above $n = 100$, in $\text{Kr}^{7+*}(n)$ ions produced after electron capture from excited $\text{Rb}^*(17p)$ Rydberg atoms. The distributions over n of the cross sections have been obtained for two collisional energies, and are compared with theoretical results based on CTMC calculations. The broad n distributions of the experimental cross sections are in reasonable agreement with the theoretical CTMC ones, as far as the overall behavior and the position of their maxima are concerned, but appear to be narrower by about a factor of 2. However, they are still much broader than those predicted by the ECB model which yields widths about 3 to 4 times narrower.

We would like to thank O. Deyris for his technical assistance, A. Brenac, G. Lambole, and T. Lamy for providing multicharged ion beams, M. Benhenni, B. Huber, and S. Martin for their collaboration in the early stage of this experiment, as well as G. Baum and N. J. van Druten. We are also grateful to F. B. Dunning,

T. F. Gallagher, E. Luc-Koenig, K. B. MacAdam, R. E. Olson, and C. O. Reinhold for fruitful discussions. The AIM/ex-LAGRIPPA is a joint facility of the Commissariat à l'Énergie Atomique (CEA) and of the Centre National de la Recherche Scientifique (CNRS).

-
- [1] R. E. Ryufuku, K. Sasaki, and T. Watanabe, *Phys. Rev. A* **21**, 745 (1980).
 - [2] R. G. Rolfes and K. B. MacAdam, *Phys. Rev. A* **15**, 4591 (1982); K. B. MacAdam, L. G. Gray, and R. G. Rolfes, *ibid.* **42**, 5269 (1990).
 - [3] S. Schippers, A. R. Schlatmann, W. P. Wiersema, R. Hoekstra, R. Morgenstern, R. E. Olson, and J. Pascale, *Phys. Rev. Lett.* **72**, 1628 (1994).
 - [4] M. Gieler, F. Aumayr, J. Schweinzer, W. Koppensteiner, W. Husinsky, H. P. Winter, K. Lozhkin, and J. P. Hansen, *J. Phys. B* **26**, 2137 (1993).
 - [5] R. E. Olson, *J. Phys. B* **13**, 843 (1980); J. Pascale, R. E. Olson, and C. O. Reinhold, *Phys. Rev. A* **42**, 5305 (1990).
 - [6] E. Jacquet, P. Boduch, M. Chantepie, M. Druetta, D. Hennecart, X. Husson, D. Lecler, F. Martin-Brunetière, R. E. Olson, J. Pascale, and M. Wilson, *Phys. Scr.* **49**, 154 (1994).
 - [7] T. Lamy, G. Lambole, D. Hitz, and H. J. Andrä, *Rev. Sci. Instrum.* **61**, 336 (1990).
 - [8] S. Runge, A. Pesnelle, M. Perdrix, D. Sevin, N. Wolffer, and G. Watel, *Opt. Commun.* **42**, 45 (1982).
 - [9] P. Pillet, H. B. van Linden van den Heuvell, W. W. Smith, R. Kachru, N. H. Tran, and T. F. Gallagher, *Phys. Rev. A* **30**, 280 (1984).
 - [10] A. Niehaus, *J. Phys. B* **19**, 2925 (1986).
 - [11] R. J. Damburg and V. V. Kolosov, in *Rydberg States of Atoms and Molecules*, edited by R. F. Stebbings and F. B. Dunning (Cambridge University Press, Cambridge, 1983), p. 31.
 - [12] T. F. Gallagher, L. M. Humphrey, W. E. Cooke, R. M. Hill, and S. A. Edelstein, *Phys. Rev. A* **16**, 1098 (1977); T. J. Jeys, G. W. Foltz, K. A. Smith, E. J. Beiting, F. G. Kellert, F. B. Dunning, and R. F. Stebbings, *Phys. Rev. Lett.* **44**, 390 (1980).
 - [13] H. A. Bethe and E. E. Salpeter, *Quantum Mechanics of One- and Two-Electron Atoms* (Plenum Publishing Corporation, New York, 1977), p. 266.
 - [14] A. Lindgard and S. E. Nielsen, *At. Data Nucl. Data Tables* **19**, 633 (1977).